

# Influence of Hoek-Brown linearization and input cross-correlation in slope Probability of Failure Calculation

CE Valderrama, F Sanz and E Hormazábal  
*SRK Consulting Chile, Santiago, Chile*

## Abstract

When Hoek-Brown failure-criterion (H-B) is selected, their parameters are determined as the ones that better fit data; therefore, depends on the method of fitting, the experimental error and statistical sufficiency of data. If these uncertainties are considered, H-B parameters are random variables. On the other hand, in slope stability analyses, is common to linearize the H-B criterion to estimate equivalent friction angle,  $\phi_e$ , and cohesion,  $c_e$ , which generate a non-linear relation between  $\phi_e$  and  $c_e$ . In this paper, we examine the effect of this linearization in probabilistic analyses that use a Mohr-Coulomb criterion when the input data are random H-B parameters. We study the uncertainty propagation from H-B parameters to  $\phi_e$  and  $c_e$ . Additionally, because linearization cross-correlate  $\phi_e$  and  $c_e$ , we analyze the effect of the correlation  $\rho_{\phi c}$  in Factor of Safety (FS) and Probability of Failure (PoF) results, finally because also H-B parameters can be correlated we examine the effects on FS and PoF.

## 1. Introduction

Properties of geotechnical materials are affected by various factors during their formation process, such as properties of parent materials, magmatism, sedimentation, weathering, erosion processes, and therefore, vary spatially. Additionally, several uncertainties are incorporated in the estimation of the properties as result of imperfect test equipment and procedural errors, statistical uncertainty arising from insufficient number of tests, and the transformation uncertainty related to the interpretation of results (Cao et al., 2017). For example, if Hoek-Brown rock mass failure criterion is adopted, there is error and variability associated to the results of triaxial and unconfined compressive tests, and the number of available tests is commonly restricted. Also, the values of the parameters depend on the method of fitting (e.g. non-linear least squares or Bayesian sampling, absolute residual or relative residual, etc.)

Probability theory and statistics gives a framework to rationally incorporate these uncertainties into geotechnical analysis, allowing to measure the performance of geotechnical structures statistically, for example, through the reliability index,  $\beta$ , and the probability of failure, PoF. The last one, defined as the probability of performance requirements not be-

ing satisfied, has grown in use as an acceptance criterion because combined with risk assessment is a good option to deal with uncertainty and variability, and several methods have been proposed to estimate it, such as the first-order second-moment method (Christian et al., 1974; Hassan & Wolff, 1999), the first-order reliability method (Low et al., 1988; Low, 2003), response surface methods (Morgan & Henrion, 1990 and Tandjiria et al., 2000) and direct Monte Carlo simulation method (Griffiths & Fenton, 2004; El Ramly, 2005). The response surface method has been used in risk-based slope design applications as described by Steffen *et al.* (2008) and Contreras (2015). This approach has the advantage of combining the rigor of a Monte Carlo simulation with the practicality of requiring fewer FS calculations with the geotechnical model to construct the response surface used as a surrogate model in the process.

On the other hand, for rock masses is generally accepted to use non-linear Hoek-Brown (H-B) failure envelopes. Hoek (2007) recommends, where possible, to apply the criterion directly; however, given that many geotechnical design calculations are written for the Mohr-Coulomb failure criterion (M-C), it is often necessary to calculate equivalent rock mass cohesion,  $c_e$ , and friction,  $\phi_e$  (Eberhardt, 2012). This is particularly true in rock slope analyses, for example, to include the weakness induced by joints, it is

common to use a linear weighing of the strength contributed by the rock mass and joints fractions of material (e.g. Jennings, 1970); therefore, linear failure envelopes, as the Mohr-Coulomb criterion, are used to represent equivalent strength.

The linearization of H-B criterion is done by fitting an average linear relationship to the H-B curve in the range  $\sigma_t < \sigma_3 < \sigma_{3max}$ , process which involves balancing the areas above and below the M-C plot (Hoek et al., 2002). The output of this process are explicit expressions for  $\phi_e$  and  $c_e$  in terms of H-B parameters ( $a$ ,  $s$ ,  $m_b$ ,  $\sigma_{ci}$ , GSI, D) and  $\sigma_{3max}$ . As a result, the linearization of H-B parameters implies a non-linear relation between  $\phi_e$  and  $c_e$ .

If H-B parameters are considered as random variables, the linearization operation propagates their uncertainties (intrinsic to their distributions), generating random variables  $\Phi$  (friction) and  $C$  (cohesion) for which we do not know their distributions a priori, but we know that are correlated.

However, because lack of data, it is common to assume that strength properties are independent random variables. If a Mohr-Coulomb (M-C) failure criterion is used to model the material failure envelope, this means that friction angle ( $\phi$ ) and cohesion ( $c$ ) are considered independent; however, cross-correlation between  $\phi$  and  $c$  has been widely reported (e.g. Young, 1986; Di Matteo et al., 2013), and ignoring their cross-correlation may lead to the underestimation or overestimation of the failure probability (e.g. Jiang et al., 2014; Wu, 2013; Johari & Mehrabani Lari, 2017). Other option is to use linear correlations between  $\phi$ - $c$ , which can be obtained through laboratory tests, but normally the available information is not enough to statistically define this coefficient.

Furthermore, the H-B random variables can also be correlated to each other, as for example the reasonable correlation between the ratio  $\sigma_{ci}/\sigma_t$  and the parameter  $m_i$  (Sheorey, 1997); therefore, in the same sense that for M-C criterion, neglecting cross-correlation between H-B parameters could generate underestimation or overestimation of PoF.

For this reason, in this paper we study the uncertainty propagation from Hoek-Brown parameters to  $\phi_e$  and  $c_e$ , i.e. we study the distributions of random variables  $\Phi$  (friction) and  $C$  (cohesion) obtained from the H-B linearization; the influence of  $\phi_e$ - $c_e$  cross-correlation induced by linearization in the FS and PoF, and finally, we study the effect of the correlation of H-B parameters in FS and PoF.

This paper is organized as follow: Section 2 outlines the methodology used along this paper. Section 3 shows the obtained results and the analysis of them, and finally, in Section 4 the conclusions of this work are presented.

## 2. Methodology

The scheme of the work of this paper is shown in Figure 1. The first step consists in to generate random variables for friction  $\Phi$  and cohesion  $C$ , that comes from linearization of Hoek-Brown parameters, which are in turn, correlated random variables. For simplicity, we select  $m_i$  and  $\sigma_{ci}$  as random variables (M and S), and the other properties which not depend on them (GSI, D) are considered as constants.

Uniform and normal probability density functions (pdf) were considered for M and S. The former one because is the pdf with largest entropy, i.e. minimizes the information assumed into the distribution, while the later one because is the commonly found distribution for data. M and S distributions are generated with specific correlations  $\rho_{MS}$ , imposed by means of Gaussian copulas. Linearization of M and S generate distributions of  $\Phi$  and  $C$ . At this point, we study the effect of  $\rho_{MS}$  over the distribution of  $\Phi$  and  $C$ .

Pairs of discrete values of  $\phi_e$  and  $c_e$ , with correlation coefficient  $\rho_{\phi c}$  induced by the linearization, are used to calculate discrete values of FS. By doing this a large number of times, we can study the distribution of FS and obtain the PoF as the number of simulations with  $FS < 1$  divided by total number of simulations. Additionally, we make Monte Carlo simulations over  $\Phi$  and  $C$  to obtain pairs  $(\phi_e, c_e)$  with different correlation coefficients  $\rho_{\phi c}$ . With this new re-sampling we calculate FS and study the influence of  $\rho_{\phi c}$  in PoF. Finally, we change the values of  $\rho_{MS}$  to observe its influence in FS and PoF.

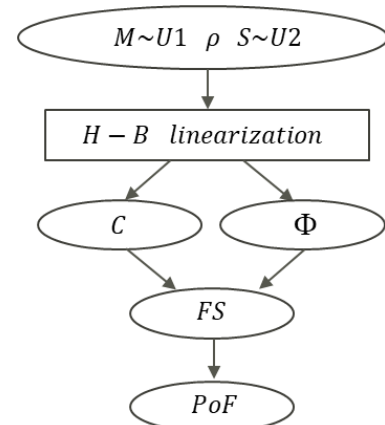


Figure 1. Scheme which summarized the work done in this paper. From correlated H-B properties, M-C properties are obtained and the effects on FS and PoF are studied.

Because PoF evaluation implies the calculation of thousands of FS computations, FS were calculated by means of the Equation (1) (Carranza-Torres & Hormazábal, 2018), allowing a quick calculation of PoF. Additionally, to have an explicit expression for the Factor of Safety can be advantageous during the analysis of the results:

$$\frac{FS}{\tan \phi} = \frac{1}{\tan \alpha} + \frac{g_1(\alpha)}{X_{ad}} + \frac{g_2(\alpha)}{X_{ad}g_3(\alpha)} \quad (1)$$

Where  $X_{ad}$  is the dimensionless parameter given by Equation (2), and  $g_i(\alpha)$  are cubic polynomials of the slope angle given in detail in Carranza-Torres & Hormazábal (2018).

$$X_{ad} = \frac{\gamma H \tan \phi}{c} \quad (2)$$

Hence, Equation (1) depends on cohesion ( $c$ ), friction angle ( $\phi$ ), slope height ( $H$ ), unit weight ( $\gamma$ ) and slope angle ( $\alpha$ ), and is valid for slopes of arbitrary height and inclination in homogeneous/isotropic dry ground, that obeys the Mohr-Coulomb shear failure criterion.

### 3. Results

#### 3.1 Effect of linearization to $C$ and $\Phi$

The objective of this section is to obtain an idea of how variability of  $m_i$  and  $\sigma_{ci}$ , represented by the random variables  $M$  and  $S$ , is propagated by the linearization in the random variables  $C$  and  $\Phi$ :

$$L(M, S) \rightarrow (C, \phi) \quad (3)$$

Where  $L$  represents linearization operation. Figure 2 shows how  $(m_i, \sigma_{ci})$  points obtained from uniform (a right side) and normal truncated (at left side) distributions are mapped into  $\phi_e - c_e$  space by  $L$ . Red colors identify zones with more density of points. The spatial bounds of  $\phi_e - c_e$  are clearly non-linear, and there is a strong loss of symmetry in their distribution; therefore, the obtained probability density functions for  $C$  and  $\Phi$  have skewness, as shown in Figure 3, where it is possible to see a normalized histogram of  $\phi_e$  obtained from uniform distributed  $M$  and  $S$ .

Several runs were done for different ranges of  $m_i, \sigma_{ci}$ , where minimum, maximum and mean distribution values were selected randomly. We observe the behavior of the obtained distributions in terms of their 'shape', and their first, second and third moments. We made the following general conclusions:

- There is a great variability in the resulting distributions  $C$  and  $\Phi$  depending for example in the range of input values  $m_i, \sigma_{ci}$ . Hence, is not possible (the option of an analytical calculation was not considered in this study) to indicate a close expression for the resulting distributions and their parameters.
- As expected (see Eberhardt, 2012), sample means of  $M$  have a positive correlation with sample means of  $\Phi$ , while  $S$  is correlated with  $C$ .  $M$  and  $C$  appears uncorrelated, same that  $S$  and  $\Phi$ . The effect of correlation  $\rho_{MS}$  is negligible.
- The same as above was observed for variances. It was also observed that when  $M$  variance increase, the statistical dispersion of  $\Phi$  is also increased (Figure 2). The same for  $S$  and  $C$ .
- $C$  and  $\Phi$  are truncated pdf. This behavior is expected because  $M$  and  $S$  are also truncated pdf.
- In general, the shape of the obtained pdfs,  $C$  and  $\Phi$ , are similar to the 'root' pdfs,  $M$  and  $S$ , i.e. if  $M$  and  $S$  distributed as uniform, then  $C$  and  $\Phi$  distribute as uniform; however, as variance of  $M$  and  $S$  increase, skewness also increases in  $C$  and  $\Phi$ , where  $C$  is more prone to suffer positive skewness, while  $\Phi$  negative skewness (see Figure 4).
- When  $\rho_{MS} = 0$ ,  $C$  and  $\Phi$  are more prone to distribute as normal.

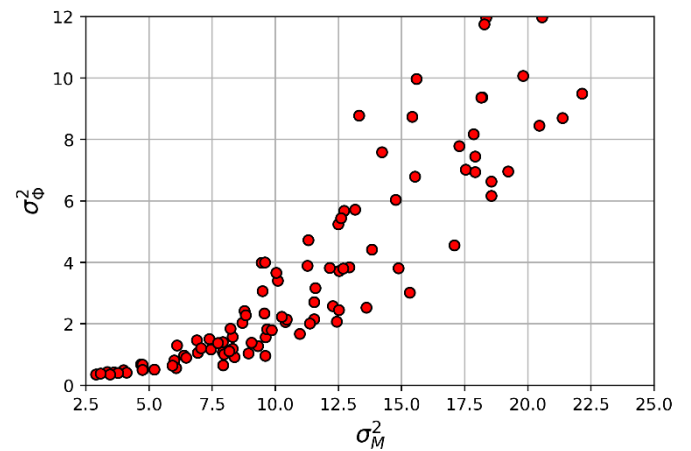


Figure 2. Comparison of variances of  $M$  and  $\Phi$ . It is observed that variance of  $\Phi$ (output) increase when variance of  $M$  (input) increase. The statistical dispersion is also increased when variance of  $M$  increase.

Therefore, if variabilities of  $m_i, \sigma_{ci}$  are non-negligible, it is necessary to incorporate their effect in



probabilistic analyses, calculating their means, variances, verify how correct is the use of symmetric distributions of  $C$  and  $\Phi$ , etc. A Monte Carlo simulation appears as a simple method to study the statistical characteristics of  $C$  and  $\Phi$ .

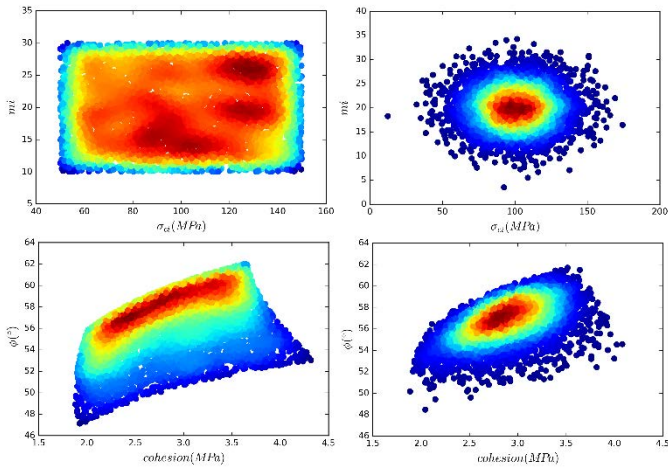


Figure 3. Scatter plots of discrete points of  $(m_i, \sigma_{ci})$  and  $(\phi_e, c_e)$  where red color represent more density. At the upper left side,  $(m_i, \sigma_{ci})$  points obtained from uniform distribution and below him, the corresponding points  $(\phi_e, c_e)$ . At the right side,  $(m_i, \sigma_{ci})$  points obtained from normal distribution and the corresponding  $(\phi_e, c_e)$  points.

It is important to mention that pairs  $(\phi_e, c_e)$  obtained from linearization of H-B, and used to construct  $C$  and  $\Phi$ , are correlated and follows a non-linear relation. We can be tempted to use these probability distributions of  $C$  and  $\Phi$ , like the one in Figure 4, and calculate PoF without considering their correlation  $\rho_{\phi c}$  (e.g. by a MonteCarlo simulation), but this procedure could generate an error in PoF calculation. In fact, the use of the linear Pearson correlation coefficient could be inadequate to characterize the correlation between  $\phi_e$  and  $c_e$ , due to a marked non-linear behavior, and a different correlation coefficient, as the distance correlation (Szekely et al., 2007), could be better to represent how  $c$  and  $\phi$  are related.

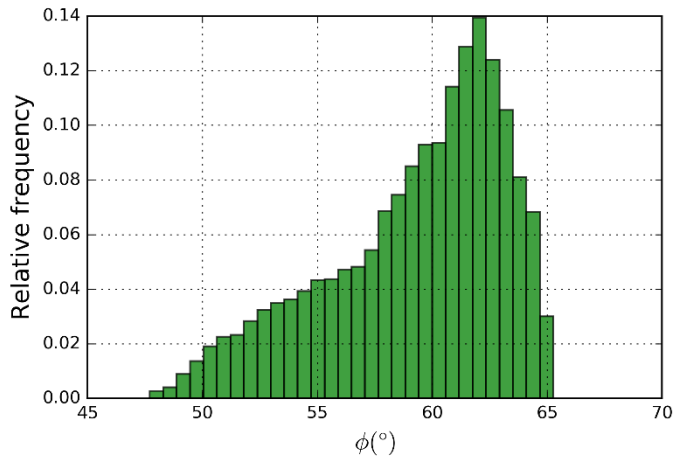


Figure 4. Normalized histogram of  $\phi_e$ , representing  $\Phi$  distribution, that was obtained from uniform distributions of  $M$  and  $S$ , showing positive skewness.

### 3.2 Effect of $\rho_{MS}$ on PoF

Because  $m_i$  and  $\sigma_{ci}$  are the variables of interest, fixed values of  $H=250m$ ,  $\beta=55^\circ$ ,  $\gamma=27kN/m^3$ , and  $r_u=0.5$  were considered in Equation (1). On the other hand, to calculate the equivalent friction and cohesion, a  $GSI=40$  and  $D=0.7$  were used (the epistemic uncertainty in these last parameters was not considered in this study, because it is focused in the variables with natural variability (Baecher & Christian, 2003), but their incorporation is an ongoing work). The FS function obtained with Equation (1) is shown as contour plot in Figure 5.

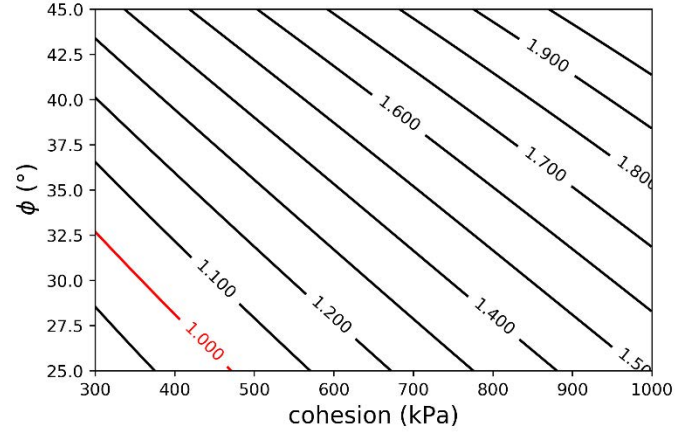


Figure 5. Contour plot representation of the Factor of Safety obtained with the Equation (1) (Carranza-Torres and Hormazabal, 2018) in terms of cohesion and friction. Red line shows the iso-contour of  $FS=1$ .

Clearly, it is non-common to have an explicit representation for the FS as Figure 5; however, we can take advantage of this to better understand the influence of  $\rho_{MS}$  in PoF. Figure 6 shows the location of 4,000 pairs  $(c, \phi)$ , where the red ones were obtained from linearization, and the blue ones represent uncorrelated data ( $\rho_{\phi c}=0$ ).

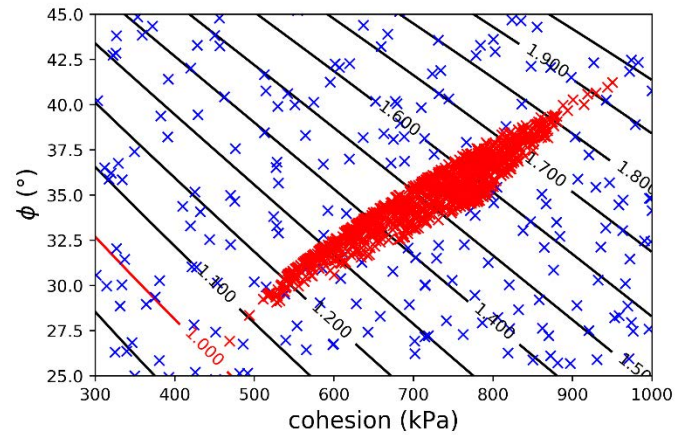


Figure 6. Random pairs  $(c, \phi)$  over the contour representation of FS. In blue, uncorrelated points, while red points represent correlation points obtained from H-B linearization.

For uncorrelated data ( $\rho_{\phi c}=0$ ), all the pairs  $(c,\phi)$  in range  $R_c \times R_\phi$  (where  $R_i=[i_{\min},i_{\max}]$ ) have the same probability to occur; therefore, the PoF can be interpreted as the ratio between the area in which  $FS<1$  and the total area  $R_c \times R_\phi$ :

$$PoF(\rho_{c\phi} = 0) \approx \frac{\int_{R_c} \int_{R_\phi} H(-FS(c,\phi)) dc d\phi}{R_c R_\phi} \quad (4)$$

Where  $H(\cdot)$  is the Heaviside function. On the other hand, Figure 6 shows that linearization restricts the area of feasible pairs  $(c,\phi)$ . In this case PoF could be calculated similarly to the former case as:

$$PoF(\text{lin}) \approx (\int_{\omega} H(-FS(c,\phi)) d\omega) / (\int_{\omega} d\omega) \quad (5)$$

Where  $\omega$  is the region of feasible pairs  $(c_e, \phi_e)$ . Therefore, the correlation between  $M$  and  $S$ ,  $\rho_{MS}$ , modifies at first the set of possible values for  $m_i$  and  $\sigma_{ci}$ . Figure 7 shows in scatter plots, the sets of possible values of  $m_i$  and  $\sigma_{ci}$  obtained for a negative correlation  $\rho_{MS}=-0.9$ .

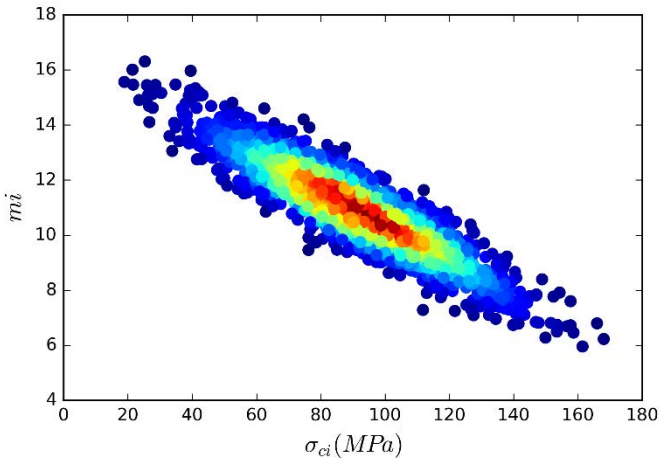


Figure 7. Scatter plots of the set of possible values of  $m_i$  and  $\sigma_{ci}$  for  $\rho_{MS}=-1$ .

This effect impact directly in the set of feasible values of pairs  $(c, \phi)$ , and therefore, in the results of PoF. To evaluate the effect of the correlation Figure 8 shows PoF results obtained for different values of correlation  $\rho_{MS}$ . It is observed that for this case, PoF increase when the correlation is positive, and decrease when correlation is negative, existing a difference of 8% between minimum and maximum values of PoF. In the case  $\rho_{MS}=-1$  the region of feasible values of  $c$  and  $\phi$ , must be near to parallel to the iso-contours of  $FS=1$  (see Figure 5) and to be above of the iso-contour  $FS=1$ , which explains the PoF near to zero. On the other

hand, the region of feasible points  $\rho_{MS}=1$  is near to perpendicular to iso contours, which explains that the maximum values of PoF are encounter for this value of  $\rho_{MS}$ ; however, this behavior cannot be generalized, and each case needs to be analyzed separately.

These results indicate that this correlation is an important input in probabilistic studies and needs to be considered, and a possible way to do it is by means of Bayesian methods as in Contreras et al. (2016).

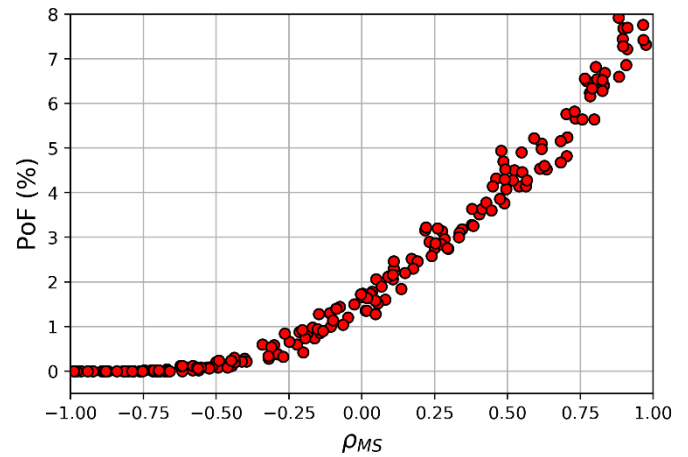


Figure 8. Effect of  $\rho_{MS}$  on PoF.

## 4. Conclusions

In this paper, we analyze the effect of the linearization of Hoek-Brown criterion commonly done in slope stability, into Factor of Safety and Probability of Failure calculations, considering parameters  $m_i$  and  $\sigma_{ci}$  as random variables.

First, we observe that H-B linearization generates skewness in the distributions of  $c$  and  $\phi$ , and therefore, considering symmetric distributions  $C$  and  $\Phi$  could induce inaccuracies in results.

The correlation induced by H-B linearization needs to be considered, because PoF results depend greatly of the correlation of  $c, \phi$ . Therefore, pairs of points  $(c, \phi)$  generated during linearization must be used for FS calculations, and no pairs  $(c, \phi)$  randomly sampled from pdf's  $C$  and  $\Phi$ , for example by Monte Carlo.

Depending on the range of  $m_i$  and  $\sigma_{ci}$ , the correlation coefficient of  $c$  and  $\phi$  after linearization varies from -1 to 1. Sometimes, non-linear relation is found between  $c$  and  $\phi$ , which indicate that it is better to use a correlation measurement different that the classical Pearson correlation (linear).

Finally, it was observed that the correlation between the inputs H-B parameters also has an important effect in PoF results. This correlation is difficult to measure, because depends, for example, in the method of fitting of experimental points, but if exists can have a non-negligible effect in results.

It is important to mention that GSI and D parameters, which have an important effect in equivalent cohesion and friction were not considered in this study, but their influence is an ongoing work.

## 5. References

- Baecher GB and Christian JT. (2003). *Reliability and Statistics in Geotechnical Engineering*, Chichester, Wiley.
- Cao Z, Wang Y and Li D. (2017). *Probabilistic Approaches for Geotechnical Site Characterization and Slope Stability Analysis*. Berlin, Springer-Verlag, 190pp.
- Carranza-Torres and Hormazábal E. (2018). Computational tools for the determination of factor of safety and location of the critical circular failure surface for slopes in Mohr-Coulomb dry ground. *Proc. of Slope Stability Symposium 2018, Sevilla, Spain*.
- Christian JT, Ladd CC and Baecher GB. (1994). Reliability applied to slope stability analysis. *Journal of Geotechnical Engineering* 120(12): 2180-2207.
- Contreras, LF. (2015). An economic risk evaluation approach for pit slope optimization. *The Journal of The Southern African Institute of Mining and Metallurgy*, 115.
- Contreras, LF. Brown ET and Ruest M. (2018). Bayesian data analysis to quantify the uncertainty of intact rock strength. *Journal of Rock Mechanics and Geotechnical Engineering* 10:11-31.
- Di Matteo L, Valigi D and Ricco R. (2013). Laboratory shear strength parameters of cohesive soils: variability and potential effects on slope stability. *Bull. Eng. Geol. Environ.* 72(1): 101-106.
- Eberhardt, E. (2012). The Hoek-Brown failure criterion. *Rock. Mech. Rock Eng.* 45: 981-988.
- El-Ramly H, Morgenstern NR, Cruden DM. (2005). Probabilistic assessment of stability of a cut slope in residual soil. *Geotechnique* 55(1): 77-84.
- Griffiths DV and Fenton GA. (2004). Probabilistic slope stability analysis by finite elements. *J. Geotech. and Geonviron. Eng.* 130(5): 507-518.
- Hassan AM and Wolff TF. (1999). Search algorithm for minimum reliability index of earth slopes. *Journal of Geotechnical and Geoenvironmental Engineering* 125(4): 301-308.
- Hoek E, Carranza-Torres C and Corkum B. (2002). Hoek-Brown failure criterion – 2002 edition. In: Hammah R, Bawden W, Curran J, Telesnicki M (eds) *Proc. 5th North American Rock Mechanics Symposium*. Toronto, University of Toronto Press, 267-273.
- Hoek E. (2007). *Practical Rock Engineering*. e-Book, Rocscience, 341pp.
- Jiang SH, Li DQ, Cao ZJ and Zhou CB. (2014). Efficient system reliability analysis of slope stability in spatially variable soils using Monte Carlo simulation. *J. Geotech. Geonviron. Eng.* 141(2): 1-13.
- Jennings JE. (1970). A mathematical theory for the calculation of the stability of open cast mines. *Proc. of the Symposium on Theoretical Background to the Planning of Open Pit Mines, Johannesburg, SA*, 87-102.
- Johari A & Mehrabani Lari A. (2017). System probabilistic model of rock slope stability considering correlated failure modes. *Computers and Geotechnics* 81: 26-38.
- Low BK, Gilbert RB and Wright SG. (1998). Slope reliability analysis using generalized method of slices. *Journal of Geotechnical and Geoenvironmental Engineering* 34(5): 672-685.
- Low BK. (2003). Practical probabilistic slope stability analysis. *Proc. 12th Panamerican Conference in Soil Mechanics and Geotechnical Engineering, Cambridge, Massachusetts, USA*, 2777-2784.
- Morgan, M.G. and M. Henrion. 1990. Uncertainty: a guide to dealing with uncertainty in quantitative risk and policy analysis. Cambridge University Press.
- Sheorey PR. (1997). *Empirical Rock Failure Criteria*. Rotterdam: Balkema.
- Steffen, O.K.H., Contreras, L.F., Terbrugge, P. J. & Venter, J. (2008). A Risk Evaluation Approach for Pit Slope Design. *Proceedings of the 42nd US Rock Mechanics Symposium and 2nd U.S.-Canada Rock Mechanics Symposium, San Francisco, USA*, June 29-July 2.
- Tandjiria V, Teh CI and Low BK. Reliability analysis of laterally loaded piles using response surface methods. *Structural Safety* 22: 335-355.
- Wu XZ. (2013). Trivariate analysis of soil ranking-correlated characteristics and its application to probabilistic stability assessments in geotechnical engineering problems. *Soils Found.* 53(4), 540-556.
- Young DS. (1986). A generalized probabilistic approach for slope analysis: practical application to an open pit iron mine. *Int. J. Min. Geol. Eng.* 4(1):3-13.